Liquid-Crystalline Phases of Cholesterol/Lipid Bilayers as Revealed by the Fluorescence of *trans*-Parinaric Acid

C. Reyes Mateo,* A. Ulises Acuña,* and Jean-Claude Brochon‡

*Instituto de Quimica-Fisica "Rocasolano," CSIC, E-28006 Madrid, Spain, and ‡Laboratoire de Biochimie Moléculaire et Cellulaire, URA 1131 CNRS, Université Paris Sud, F-91405 Orsay, France

ABSTRACT   The presence of two liquid-crystalline phases, α and β, in mixed bilayers of dimyristoylphosphatidylcholine/cholesterol was detected by the changes in the distribution of the fluorescence lifetimes of t-PnA, as analyzed by the Maximum Entropy Method. The formation of the liquid-ordered β-phase, in the 30–40°C temperature range as a function of cholesterol concentration (0–40 mol%), could be related quantitatively to the relative amplitude of a long lifetime component of the probe (10–14 ns). Based on this evidence, the phase behavior of mixtures of the unsaturated lipid palmitoyloleoylphosphatidylcholine and cholesterol was determined using the same technique, for cholesterol concentrations in the 0–50 mol% range, between 10 and 40°C. It was found that two liquid-crystalline phases are also formed in this system, with physical properties reminiscent of the α- and β-phases formed with saturated lipids. However, in this case it was determined that, for temperatures in the physiological range, the α- and β-phases coexist up to 40 mol% cholesterol. This finding may be of significant biological relevance, because it supports the long held notion that cholesterol is responsible for the lipid packing heterogeneity of several natural membranes rich in unsaturated lipid components.

INTRODUCTION

Cholesterol is an important constituent of the lipid bilayer of plasma membranes of eukaryotic cells, and its role in modulating the physical properties of the bilayer has been the subject of intense investigation over the past two decades. Many of these studies have been carried out in phospholipid:cholesterol model systems using several physical methods such as ^{2}H-NMR spectroscopy (Vist and Davis, 1990; Thewalt and Bloom, 1992; Reinl et al., 1992; Linseisen et al., 1993), EPR (Recktenwald and McConnell, 1981; Pasenkiewicz-Gierula et al., 1990; Sankaram and Thompson, 1990, 1991), stationary and time-resolved fluorescence spectroscopy (Lentz et al., 1980; Gallay and Vincent, 1986; Schroeder et al., 1990; Almeida et al., 1992; Parasassi et al., 1994), neutron scattering (Mortensen et al., 1988) and DSC (Mabrey et al., 1978; Vist and Davis, 1990), as well as theoretical approaches (Ipsen et al., 1987, 1990; Scott, 1991). From these efforts, it has been established to a reasonable degree of certainty that mixtures of cholesterol and saturated phospholipids, such as dipalmitoylphosphatidylcholine (DPPC) and dimyristoylphosphatidylcholine (DMPC), produce two temperature-dependent liquid-crystalline phases that coexist for cholesterol concentrations of 10 to 25–30 mol%: a liquid-disordered (α)-phase and a liquid-ordered (β)-phase (Fig. 1, after Almeida et al., 1992). At higher cholesterol concentrations, the structure of the bilayer corresponds to that of the β-phase over a large temperature range. The β-phase is characterized by rather unique properties such as, e.g., a highly ordered distribution of lipids that, in contrast, exhibit fast-

translational and rotational mobility (Bloom et al., 1991). Because most plasma membranes contain cholesterol at a concentration higher than 30 mol%, it has been proposed that the β-phase would be a good model of the state of bulk lipid in natural plasma membranes.

A majority of the hydrocarbon chains in the membranes of eukaryotic cells have a varying degree of unsaturation. Therefore, model bilayers made up of mixtures of cholesterol and unsaturated phospholipids (such as palmitoyloleoylphosphatidylcholine (POPC), for instance) should provide a closer analog to the natural system than those with saturated lipids. However, there are few previous studies on the phase properties of such mixtures. Recently, Thewalt and Bloom (1992) and Linseisen et al. (1993) have investigated mixtures of POPC/cholesterol and stearoylelaidoylphosphatidylcholine (SEPC)/cholesterol, respectively, using ^{2}H-NMR techniques and obtained partial phase diagrams that describe in detail phase boundaries for temperatures below the transition temperature T_m. Because above T_m the lipid exchange between α- and β-phases is too fast for the NMR time scale (Bloom et al., 1991), the phase boundaries in this range of temperatures could not been determined.

The emission from fluorescent bilayer probes occurs over picoseconds to fractions of microseconds after excitation. In this time range, the fluorescent probe does not exchange appreciably between the different lipid phases, and it is possible to record, simultaneously, the fluorescent signals corresponding to each different probe population. What is needed, as noted by Ruggiero and Hudson (1989a), is a fluorescent probe whose spectral properties depend on the structural differences between the coexisting regions. Many of the photophysical parameters of the natural fluorescent lipid *trans*-parinaric acid (t-PnA) are very sensitive to the local density of the lipid bilayers (Sklar et al., 1977; Hudson and Cavalier, 1988; Ruggiero and Hudson, 1989a). More specifically,

Hudson et al. (1986) have remarked that the addition of cholesterol to phospholipid bilayers increases the amplitude of the t-PnA long lifetime component. Recently, we used this probe to investigate the occurrence of domains in synthetic lipid bilayers (Mateo et al., 1993a). In that work, it was shown that, from a combined study of t-PnA lifetime distribution patterns, rotational relaxation rates and order parameters, it is possible to obtain semiquantitative estimates of the presence in lipid bilayers of discrete domains with characteristic order and fluidity. In the present work, we used the same spectroscopic analysis with a dual purpose. First, we wanted to determine to what extent this fluorescence probe technique can be of use in revealing the formation and structure of the cholesterol-dependent β-phase. This was carried out by investigating the photophysics of t-PnA in large unilamellar vesicles (LUV) made up with mixtures of DMPC/cholesterol, in which the relative amount of α- and β-phases is already known from previous independent information (Fig. 1). In the second part of this work, we applied this analysis of the dynamics of t-PnA fluorescence to similar experimental measurements made on LUV made up with POPC/cholesterol and thereby demonstrated that the presence of cholesterol also induces the formation of a β-phase in the unsaturated phospholipid above the T_m.

MATERIALS AND METHODS

trans-Parinaric acid, t-PnA, from Molecular Probes (Junction City, OR), was checked by both absorption and emission spectroscopy and by HPLC. DMPC was obtained from Serdary (London, Ontario, Canada), POPC and cholesterol from Sigma Chemical Co. (St Louis, MO). All lipids were used without further purification. A stock solution of t-PnA in ethanol, bubbled with nitrogen, was stored in the dark at $-20°C$ until use.

Multilamellar lipid vesicles were prepared by resuspending the appropriate amounts of dried lipid in phosphate buffer (pH 7), the suspension then being heated above the phase transition temperature and vortexed. LUV, with a mean diameter of 90 nm, were prepared from these multilamellar
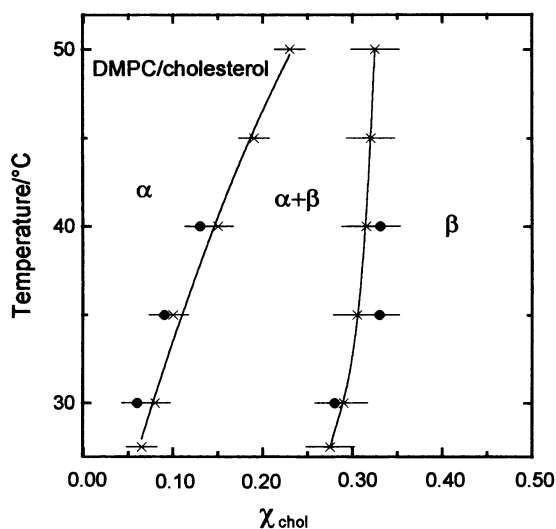

FIGURE 1 DMPC/cholesterol equilibrium phase diagram. (—×—) From Almeida et al. (1992). (●) From the t-PnA fluorescence lifetime, with a probe partition coefficient. $K_p^{\beta/\alpha} = 1.8 \pm 0.8$ (see text for details).

vesicles by pressure extrusion through Nucleopore filters with 100-nm pore size (Hope et al., 1985). The dried cholesterol-phospholipid mixtures were prepared by dissolving the weighed components in a small volume of chloroform and evaporating the solvent under a stream of nitrogen. Aliquots of t-PnA were added from the stock solution directly into the unilamellar vesicle dispersions bubbled with a stream of nitrogen. The samples were stirred at temperatures above T_m to enhance the incorporation of probe into the lipid bilayer. The final molar ratio probe/lipid was 1:100. All of the samples were prepared immediately before the spectroscopic experiments.

Steady-state fluorescence anisotropy measurements were made on an SLM 8000 spectrofluoropolarimeter (Urbana, IL) with T-format. The time-resolved total fluorescence intensity and the fluorescence anisotropy decay were obtained from the two polarized components $I_{vv}(t)$ and $I_{vh}(t)$ recorded by the time-correlated, single-photon counting technique. The excitation light pulse source was the synchrotron radiation emitted by the LURE positron storage ring at Orsay operating at a frequency of 8.33 MHz in the two-bunch mode. The storage ring provides light pulses with a full width at half-maximum (FWHM) of ≈ 500 ps. Jobin-Yvon H25 monochromators were used to select the vertically polarized excitation wavelength, at 304 and 322 nm ($\Delta\lambda = 6$ nm) and the emission wavelength at 405 nm ($\Delta\lambda = 6$ nm). The detector was a Hamamatsu R1564U microchannel plate. The instrument response function was measured for the two polarized components with a scattering silica suspension at the emission wavelength. The decay curves were stored in 2048 channels, with channel widths of 26 or 46 ps. The experimental setup is described in detail elsewhere (Brochon et al., 1993).

DATA ANALYSIS

The analysis of the total fluorescence intensity $I(t)$ was performed by the Maximum Entropy Method (MEM) (Livesey and Brochon, 1987; Brochon et al., 1992; Brochon, 1994). The parallel $I_{vv}(t)$ and perpendicular $I_{vh}(t)$ polarized components of the fluorescence intensity at time t after the start of the excitation are

$$I_{vv}(t) \tag{1}$$

$$= \frac{1}{3} E_\lambda(t) * \left[\int_0^\infty h(\tau) \cdot e^{-t/\tau} \, d\tau \left(1 + 2 \int_0^\infty \rho(\theta) e^{-t/\theta} \, d\theta \right) \right]$$

$$I_{vh}(t) \tag{2}$$

$$= \frac{1}{3} E_\lambda(t) * \left[\int_0^\infty h(\tau) \cdot e^{-t/\tau} \, d\tau \left(1 - \int_0^\infty \rho(\theta) e^{-t/\theta} \, d\theta \right) \right],$$

where $E_\lambda(t)$ is the temporal shape of the excitation flash, * denotes a convolution product, and $h(\tau)$ and $\rho(\theta)$ are the distribution functions of the fluorescence lifetimes and the rotational correlation times, respectively. The $h(\tau)$ profile is obtained from the analysis of the total fluorescence intensity $I(t)$:

$$I(t) = I_{vv}(t) + 2 \cdot I_{vh}(t) = E_\lambda(t) * \int_0^\infty h(\tau) \cdot e^{-t/\tau} \, d\tau, \tag{3}$$

One hundred lifetime values, from 0.1 to 100 ns and equally spaced on a logarithmic scale, were used for the analysis of $h(\tau)$.

The fluorescence anisotropy decay, $r(t)$, was analyzed using a Marquardt nonlinear least-squares search, by fitting simultaneously the horizontal and vertical polarized fluorescence decay traces (Gilbert, 1983; Cross and Fleming, 1984). In lipid systems where different microenvironments coexist, the fluorescence anisotropy data were fit to an

"associative" model (Ludescher et al., 1987; Ruggiero et al., 1989b; Mateo et al., 1993a) in which the lifetime parameters of the total intensity decay are specifically associated with individual anisotropy parameters. In this model, the overall $r(t)$ is approximated as due to the presence of two probe populations, which are characterized by specific fluorescence, $I_\alpha(t)$ and $I_\beta(t)$ ($I_\alpha(0) = I_\beta(0) = 1$), and anisotropy, $r_\alpha(t)$ and $r_\beta(t)$, decays, respectively. The fluorescence decay for each probe population is described by a sum of exponentials. Each individual anisotropy decay is defined by a single rotational correlation time θ and a residual anisotropy r_∞. A common value for the anisotropy at time zero $r(0)$ is assumed which, in this case, is taken as an adjustable parameter in the fitting (Ruggiero and Hudson, 1989b). The decay of the total anisotropy is a linear combination of the anisotropy functions of the two populations of the probe:

$$r(t) = f_\alpha(t)r_\alpha(t) + f_\beta(t)r_\beta(t), \qquad (4)$$

where

$$f_\beta(t) = \frac{a_\beta \cdot I_\beta(t)}{a_\beta \cdot I_\beta(t) + a_\alpha \cdot I_\alpha(t)}$$

and

$$f_\alpha(t) = \frac{a_\alpha \cdot I_\alpha(t)}{a_\beta \cdot I_\beta(t) + a_\alpha \cdot I_\alpha(t)}$$

are the time-dependent fractions of the total fluorescence $I(t)$ contributed by the probe populations a_β and a_α localized in the environments β and α, respectively.

The fraction of the β-phase, χ^β, in the bilayer can be quantified from the expression

$$K_p^{\beta/\alpha} = \frac{\chi_p^\beta/\chi^\beta}{\chi_p^\alpha/\chi^\alpha} \qquad (\chi^\alpha + \chi^\beta = 1) \qquad (5)$$

where $K_p^{\beta/\alpha}$ is the partition coefficient of the probe between the β- and α-phases, with probe concentrations defined on a mole/mole lipid basis (Sklar et al., 1980), and χ_p^β and χ_p^α are the fractions of probe localized in each environment, respectively. These fractions can be estimated from the amplitudes of the total fluorescence decay (Mateo et al., 1993a) if the radiative rate constants and extinction coefficients of the probe are known or remain the same in both phases.

The average order parameter $\langle P_2 \rangle$ of an elongated fluorescent probe with cylindrical symmetry (absorption and emission transition moments assumed parallel) for which the equilibrium angular distribution function is preserved when the molecules are pumped to the emitting state (Naqvi, 1981) is related to the residual anisotropy r_∞ in such macroscopically nonoriented vesicles systems by

$$r_\infty = r_0\langle P_2 \rangle[P_2(\cos \theta)]^2, \qquad (6)$$

where $P_2(\cos \theta)$ is the second-order Legendre polynomial for the angle θ between the transition moments and the unique (long) inertial axis of the probe.

In this work, a value of $r_0 = 0.390$ (Hudson et al., 1989) was used for t-PnA, and the angle θ was taken as $0°$ to sim-plify the analysis, although its value should be close to $20°$ (Shang et al., 1991).

RESULTS

DMPC/cholesterol bilayers

The steady-state anisotropy $\langle r \rangle$ of t-PnA in lipid bilayers made up of DMPC with cholesterol concentrations ranging from 0 to 50 mol% was determined at 22, 25, 30, 35, and 40°C (Fig. 2). The curves present a sigmoidal shape above the T_m value (24°C), tending to a plateau for cholesterol contents higher than 30 mol%. The oscillatory form of the measurements at 25°C is due to the complex interplay between lifetimes and anisotropy of the probe in situations where lipid heterogeneity is maximized.

The fluorescence intensity decay of t-PnA in mixtures of DMPC and cholesterol was measured over the temperature range of 28–40°C. In pure DMPC, the emission shows a bimodal distribution of lifetimes, as described previously (Mateo et al., 1993a). This pattern is drastically modified with increasing cholesterol concentration (Fig. 3 and Table 1; note that the tabulated data are averages of at least five experiments, whereas the figure presents a typical single set of lifetime distributions). At 5 mol% cholesterol, the bimodal lifetime distribution is still very similar to that observed in pure DMPC. However, from 10 to 30 mol% cholesterol, a new long lifetime component is observed ($\tau_3 = 10$–14 ns), with a relative amplitude that depends on the cholesterol concentration and temperature (Fig. 3). At cholesterol levels greater 30 mol%, the amplitude of τ_3 becomes maximal and the only effect of a further temperature increase is a shift of the three sets of lifetimes to shorter values (Table 2).

The anisotropy decay of t-PnA in DMPC/cholesterol mixtures was recorded at 30, 35, and 40°C. At low and high
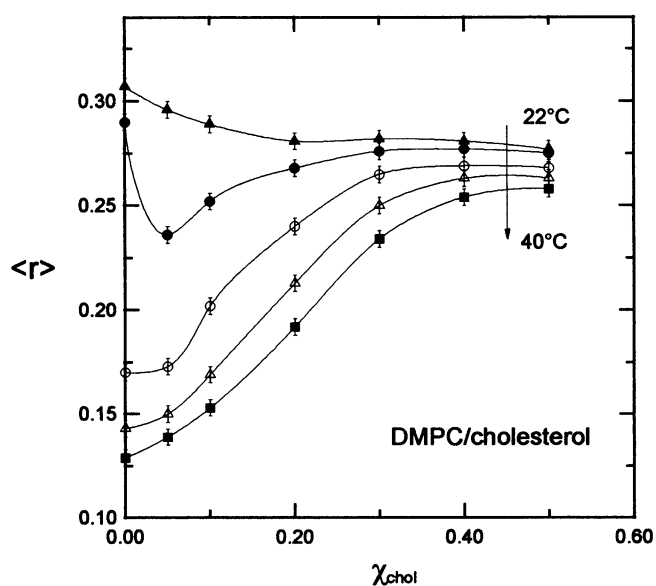

FIGURE 2 The steady-state anisotropy $\langle r \rangle$ of t-PnA in DMPC/cholesterol mixtures at 22°C (▲), 25°C (●), 30°C (○), 35°C (△), and 40°C (■) as a function of cholesterol concentration.
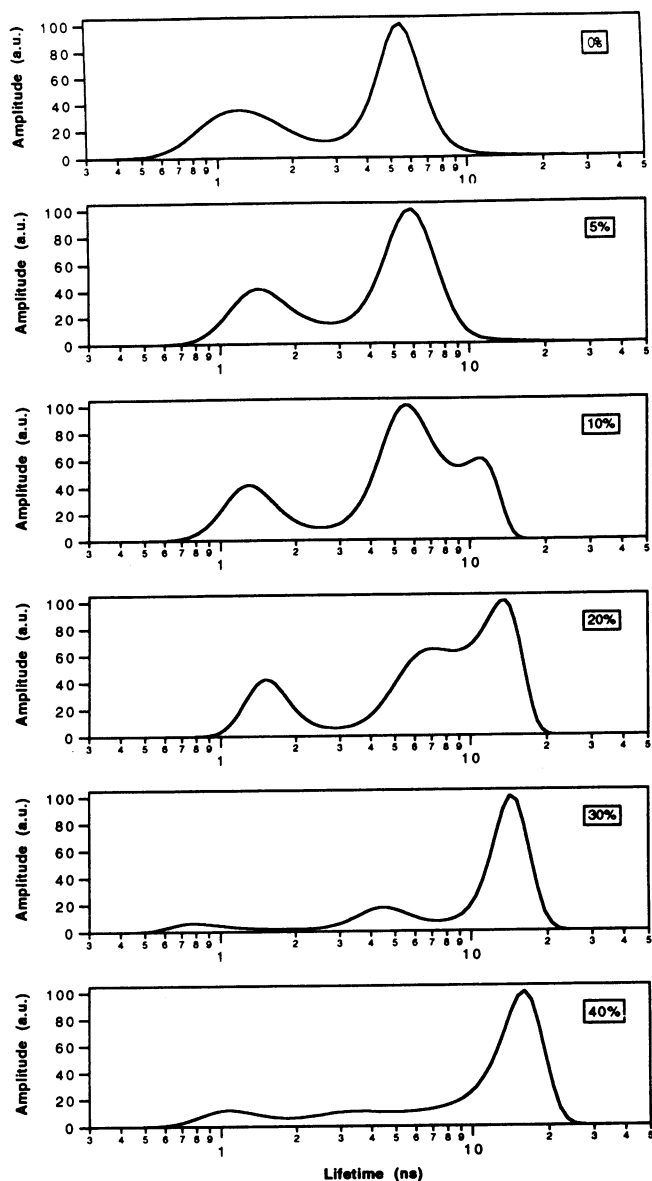
FIGURE 3   The fluorescence lifetime distribution of t-PnA in DMPC bilayers at 30°C as a function of cholesterol concentration, obtained by MEM analysis.

TABLE 1   Fluorescence intensity decay parameters of t-PnA in DMPC/cholesterol mixtures, recovered by MEM

T (°C)	X_{chol}	C_1	τ_1 (ns)	C_2	τ_2 (ns)	C_3	τ_3 (ns)
30	0.0	0.38	1.4	0.62	5.5		
	0.05	0.32	1.6	0.68	5.9		
	0.10	0.21	1.4	0.57	5.4	0.22	11
	0.15	0.17	1.5	0.44	5.6	0.39	12
	0.20	0.24	1.5	0.29	5.8	0.46	13
	0.30	0.07	0.9	0.20	4.5	0.73	14
	0.40	0.12	1.2	0.11	3.2	0.77	14
35	0.0	0.38	1.1	0.62	4.1		
	0.05	0.30	1.1	0.70	4.4		
	0.10	0.28	1.6	0.67	5.0	0.05	10
	0.15	0.23	1.1	0.53	4.7	0.24	9
	0.20	0.26	1.1	0.34	4.4	0.40	9
	0.30	0.16	1.4	0.30	6.1	0.54	12
	0.40	0.15	1.4	0.13	4.3	0.72	12
40	0.0	0.29	1.1	0.69	3.5		
	0.05	0.32	1.2	0.68	4.1		
	0.10	0.29	1.4	0.69	4.4	0.02	11
	0.15	0.25	1.4	0.56	4.6	0.19	8
	0.20	0.22	1.1	0.51	3.8	0.27	7
	0.30	0.14	1.2	0.25	3.1	0.61	8
	0.40	0.09	1.1	0.12	3.7	0.79	10

C_i and τ_i are the integrated relative amplitude and barycenter value of each lifetime class, respectively.
Average values from at least five runs.
Sample-to-sample deviations: $C_i \pm 0.04$, $\tau_1 \pm 0.2$, $\tau_2 \pm 0.8$, $\tau_3 \pm 2.0$ ns.

TABLE 2   Fluorescence intensity decay parameters of t-PnA in DMPC vesicles containing 40 mol% cholesterol as a function of temperature, recovered by MEM

X_{chol}	T (°C)	C_1	τ_1 (ns)	C_2	τ_2 (ns)	C_3	τ_3 (ns)
0.4	28	0.10	2.1	0.12	5.9	0.78	16
	30	0.12	1.2	0.11	3.2	0.77	14
	32	0.09	1.5	0.15	4.9	0.76	14
	34	0.15	2.0	0.10	4.5	0.75	13
	35	0.15	1.4	0.13	4.3	0.72	12
	37	0.14	1.4	0.14	4.3	0.72	12
	40	0.09	1.1	0.12	3.7	0.70	10
	42	0.08	1.2	0.12	3.6	0.80	10
	44	0.12	1.2	0.11	3.2	0.77	9

C_i and τ_i are the integrated relative amplitude and barycenter value of each lifetime class, respectively.
Average values from at least five runs.
Sample-to-sample deviations: $C_i \pm 0.04$, $\tau_1 \pm 0.2$, $\tau_2 \pm 0.8$, $\tau_3 \pm 2.0$ ns.

cholesterol concentration, these curves are fairly well described by a single correlation time and a residual anisotropy r_∞. However, at intermediate cholesterol concentration (Fig. 4), the curves show an increase of the anisotropy at longer time. For t-PnA this results when the probe exists in different microenvironments with characteristic individual fluorescence decay and diffusional mobility (Ludescher et al., 1987). In that case, the experimental decays were analyzed with the "associative" model described in Materials and Methods. In its simplest version, the longest lifetime component of the fluorescence distribution (Fig. 3) is associated with the fluorescence decay of the probe in the more ordered phase (β-phase), whereas the intermediate and short lifetimes are associated with the fluorescence decay of the probe

in the α-phase. The anisotropy parameters obtained from this analysis are given in Table 3.

POPC/cholesterol bilayers

The fluorescence excitation and emission spectra of t-PnA in POPC/cholesterol mixed bilayers were recorded at 20°C as a function of cholesterol concentration from 5 to 40% M. The emission spectrum remained unchanged in this range of cholesterol concentration, whereas the excitation spectrum shifted to the red by 1.5 nm when the cholesterol content was increased from 5 up to 40 mol% (data not shown).

The steady-state anisotropy $\langle r \rangle$ of t-PnA incorporated in the POPC/cholesterol mixtures was determined above
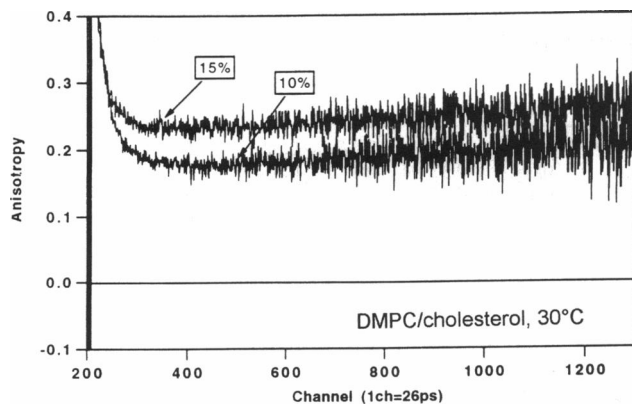
FIGURE 4   A representative decay of the fluorescence anisotropy of t-PnA in large unilamellar vesicles of DMPC for two different values of the cholesterol concentration at 30°C.

TABLE 3   Anisotropy parameters from the associative model applied to the fluorescence anisotropy decay of t-PnA in DMPC/cholesterol mixtures

T (°C)	χ_{chol}	θ^{α} (ns)	r_{∞}^{α}	θ^{β} (ns)	r_{∞}^{β}	$r(0)$
30	0.0	1.2	0.14			0.29
	0.05	0.6	0.15			0.34
	0.10	0.6	0.15	1.6	0.22	0.33
	0.15	0.4	0.16	1.4	0.24	0.34
	0.20	0.1	0.18	0.4	0.26	0.40
	0.30			0.4	0.27	0.40
	0.40			0.2	0.27	0.40
35	0.0	1.2	0.11			0.30
	0.05	0.8	0.12			0.29
	0.10	0.9	0.12	0.7	0.16	0.40
	0.15	0.6	0.15	0.7	0.21	0.35
	0.20	0.2	0.17	0.1	0.23	0.40
	0.30	0.6	0.18	0.7	0.25	0.38
	0.40			0.1	0.26	0.40
40	0.0	1.2	0.07			0.27
	0.05	0.9	0.08			0.26
	0.10	0.7	0.13			0.32
	0.15	0.7	0.12	0.2	0.18	0.31
	0.20	0.3	0.15	0.1	0.20	0.40
	0.30	0.4	0.18	0.1	0.23	0.35
	0.40			0.1	0.24	0.33

Average values from at least five runs.
Sample-to-sample deviations: $\theta^i \pm 0.2$ ns, $r_{\infty}^i \pm 0.01$.

FIGURE 5   The steady-state anisotropy $\langle r \rangle$ of t-PnA in POPC/cholesterol mixtures at 10°C (●), 20°C (○), 30°C (▲), and 40°C (△) as a function of cholesterol concentration.

shorter lifetime into two components, as previously observed (Mateo et al., 1993a, b). As in the case of DMPC, the distribution of the probe fluorescence lifetimes is very sensitive to the presence of cholesterol (Fig. 6). At a specific cholesterol concentration, a new lifetime component (τ_4) appears centered at longer times (10–16 ns). The amplitude of this component increases with increasing bilayer cholesterol content or with decreasing temperature (Table 4).

The fluorescence anisotropy decay of t-PnA in the POPC/cholesterol mixtures was recorded at 10, 20, 30, and 40°C as a function of cholesterol concentration. In this temperature range, the anisotropy decays in the subnanosecond range to a residual value r_{∞}. As in the case of DMPC, in the range of temperatures and cholesterol concentration where the fluorescence lifetime distribution showed a long lifetime component (see Table 4), the anisotropy decay was analyzed with the simplest approximation of the "associative" model with two independent probe populations. The residual anisotropies, r_{∞}^{α} and r_{∞}^{β}, determined from this analysis are included in Table 5 together with the $\chi 2$ values of the fits.

DISCUSSION

DMPC/cholesterol

In a previous related work, the kinetic parameters of the fluorescence decay of t-PnA (lifetimes and amplitudes) could be correlated with the phase composition of mixed bilayers of two saturated phospholipids DMPC/DPPC (Mateo et al., 1993a). The changes induced by temperature in the relative amount of the gel phase, as read from the phase diagram determined by differential scanning calorimetry (Mabrey and Sturtevant, 1976), corresponded closely to similar changes observed in the amplitude of the longest lifetime component of the probe fluorescence. Moreover, with the value of the gel/fluid partition coefficient of t-PnA ($K_p^{G/F} = 5 \pm 2$ (Sklar

T_m ($T_m = -5$°C) as a function of cholesterol concentration (Fig. 5). As in the case of DMPC, the isotherms show a sigmoidal shape, here with slope changes at ≈ 5 and 40 mol% cholesterol. At temperatures higher than 30°C, the discontinuities in the slope become less noticeable.

The decay of the fluorescence intensity of t-PnA in POPC/cholesterol mixtures was measured as a function of temperature from 10 to 40°C for samples with a cholesterol concentration ranging from 0 to 50 mol%. The corresponding lifetime distributions and fit parameters are shown in Fig. 6 and Table 4. In pure POPC and for a cholesterol concentration $\leq 5\%$, the curves are well described by two lifetime components at temperatures above 20°C. At the lower temperatures, the statistics of the fit is improved by splitting the
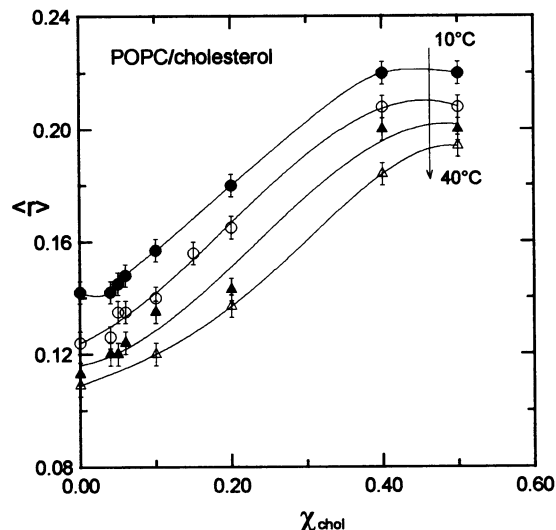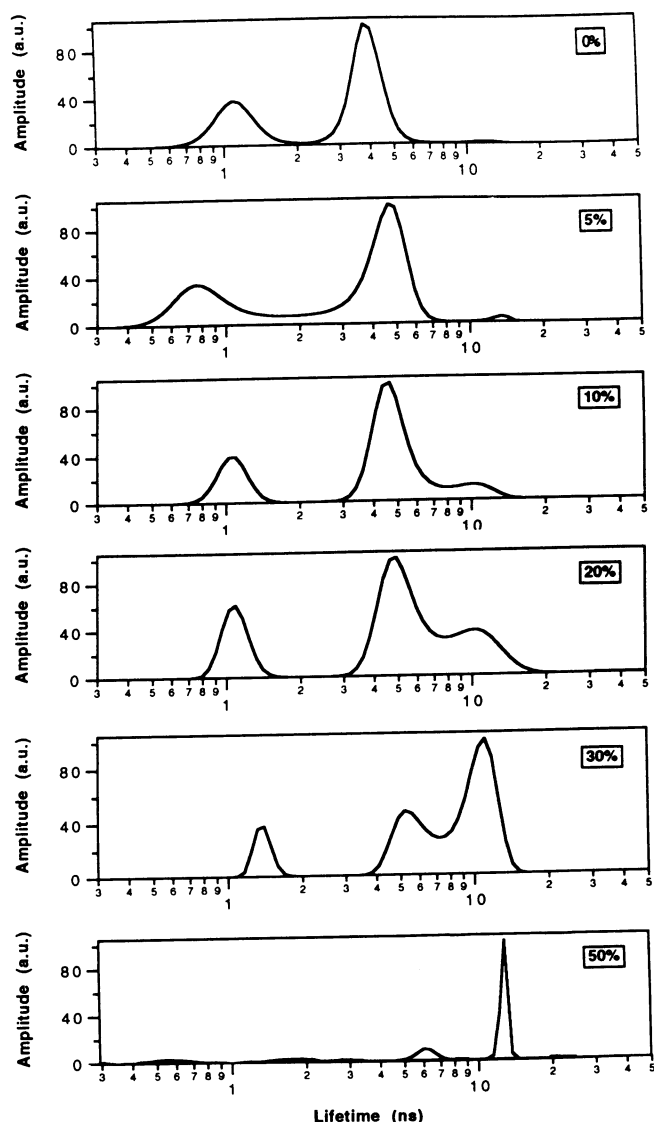
FIGURE 6 The fluorescence lifetime distribution of t-PnA in POPC at 30°C as a function of cholesterol concentration, obtained by MEM analysis.

TABLE 4 Fluorescence intensity decay parameters of t-PnA in POPC/cholesterol mixtures, recovered by MEM

T (°C)	χ_{chol}	C_1	τ_1 (ns)	C_2	τ_2 (ns)	C_3	τ_3 (ns)	C_4	τ_4 (ns)
10	0.0	0.11	1.1	0.20	3.2	0.69	9.1		
	0.05	0.20	1.1	0.16	3.7	0.33	7.5	0.31	12
	0.10	0.12	1.2	0.15	4.1	0.39	8.8	0.34	14
	0.15	0.15	1.7			0.32	7.5	0.53	15
	0.20	0.05	0.6	0.11	1.9	0.25	7.4	0.59	16
15	0.0	0.19	0.8	0.27	2.0	0.54	7.4		
	0.05	0.20	1.3	0.34	4.9	0.45	9.1		
	0.10	0.12	0.6	0.15	3.3	0.39	8.1	0.34	13
	0.20	0.16	1.9			0.34	7.1	0.50	13
	0.36	0.15	1.1			0.25	7.1	0.60	16
20	0.0	0.24	0.8	0.21	1.9	0.55	6.1		
	0.05	0.24	0.9	0.22	3.2	0.54	7.4		
	0.10	0.18	0.8	0.26	2.6	0.54	7.6	0.02	15
	0.15	0.20	1.3	0.23	3.1	0.41	7.7	0.16	12
	0.20	0.19	1.7	0.05	3.2	0.37	7.1	0.39	13
	0.30	0.23	1.1	0.06	3.2	0.24	6.8	0.47	13
	0.36	0.13	1.6			0.33	6.0	0.54	14
	0.44	0.14	1.1			0.20	6.5	0.66	15
	0.50	0.09	0.5	0.11	2.3	0.18	6.1	0.62	17
30	0.0	0.37	1.1			0.63	3.8		
	0.05	0.34	0.9			0.66	4.4	0.01	14
	0.10	0.23	1.1			0.69	4.7	0.08	10
	0.20	0.22	1.1			0.54	5.0	0.24	10
	0.30	0.14	1.3			0.46	5.6	0.40	11
	0.36	0.24	1.0			0.33	5.5	0.45	10
	0.44	0.27	0.6			0.23	5.8	0.50	11
	0.50	0.13	0.7	0.05	2.1	0.17	6.3	0.65	13
35	0.0	0.32	1.1			0.68	3.6		
	0.10	0.26	1.1			0.74	4.3		
	0.15	0.13	1.7			0.81	4.7	0.06	11
	0.20	0.18	0.9	0.15	1.8	0.56	5.0	0.11	15
	0.36	0.22	1.2			0.42	4.6	0.36	10
	0.50	0.12	1.4			0.16	4.6	0.72	9
40	0.0	0.25	1.2			0.75	2.9		
	0.05	0.37	0.9			0.63	3.1		
	0.10	0.35	0.9			0.65	3.2		
	0.20	0.30	1.3			0.67	4.5	0.03	9±1
	0.30	0.18	0.7	0.18	2.9	0.59	5.5	0.05	11±2
	0.36	0.15	1.5			0.67	4.7	0.18	13±3
	0.44	0.18	1.2			0.47	5.2	0.35	10±1
	0.50	0.09	1.2	0.04	3.0	0.41	7.4	0.46	10±1

C_i and τ_i are the integrated relative amplitude and barycenter value of each lifetime class, respectively.

Average values from at least five runs.

Sample-to-sample deviations: $C_i \pm 0.04$, $\tau_1 \pm 0.2$, $\tau_2 \pm 1.0$, $\tau_3 \pm 2.0$, $\tau_4 \pm 3.0$ ns.

et al., 1979; Sklar, 1980; Hudson et al., 1986)) and the above correlation between the long lifetime component and the gel phase, it was possible to derive a crude fluorescence version of the DMPC/DPPC thermal phase diagram.

In the case of the DMPC/cholesterol mixed bilayers studied here, the data of Table 3 and Fig. 3 show that there is a good correlation between the amount of β-phase and the amplitude of the long fluorescence lifetime component of t-PnA. For this particular lipid, the 10- to 14-ns lifetime component is first detected for cholesterol concentrations close to 10 mol%. It is interesting to note that Hudson et al. (1986) already reported the appearance of a t-PnA long lifetime component for cholesterol concentrations of 10–15 mol% in egg PC vesicles. Because the relative concentration of the α- and β-phases in the mixtures of DMPC/cholesterol is known (Fig. 1), it is possible to estimate the partition coefficient of t-PnA between the two fluid phases ($K_p^{\beta/\alpha}$) by assuming that the amplitude of the long lifetime component is proportional

to the concentration of the probe in the β-phase (see Materials and Methods). In this way, we obtained a value of $K_p^{\beta/\alpha} = 1.8 \pm 0.8$, which is significantly lower than the one determined for the partition between gel and fluid phases ($K_p^{G/F} = 5 \pm 2$). This is consistent with a structure of the β-phase much more disordered than a typical gel-phase. Further insight into the physical properties of the α- and β-phases could be obtained from the fluorescence anisotropy experiments. As was mentioned above, the decay of the t-PnA fluorescence anisotropy can be analyzed by an "associative" model in which it is assumed that the probe molecules contained in the β-phase display the long lifetime component (τ_3) only, being the two remaining shorter lifetimes (τ_1 and τ_2) associated with the probe population dissolved in the α-phase. The distribution of the probe life-

TABLE 5 Residual anisotropies r_∞ from the associative model applied to the fluorescence anisotropy decay of t-PnA in POPC/cholesterol mixtures, together with the χ^2 values obtained for each fit

T (°C)	χ_{chol}	r_∞^α	r_∞^β	$r(0)$	χ^2
10	0.0	0.10		0.28	1.10
	0.05	0.10	0.12	0.28	1.12
	0.10	0.10	0.16	0.28	1.19
	0.15	0.12	0.18	0.28	1.10
	0.20	0.14	0.20	0.29	0.99
20	0.0	0.07		0.27	1.08
	0.05	0.09		0.27	0.94
	0.10	0.11	0.15	0.33	1.02
	0.15	0.13	0.15	0.34	0.98
	0.20	0.13	0.18	0.30	0.91
	0.30	0.11	0.20	0.31	0.93
	0.40		0.23	0.34	1.03
	0.50		0.24	0.30	0.99
30	0.0	0.07		0.28	1.38
	0.05	0.08		0.29	1.19
	0.10	0.10	0.13	0.29	1.02
	0.20	0.13	0.16	0.30	0.91
	0.30	0.14	0.18	0.30	0.93
	0.40	0.16	0.22	0.31	1.03
	0.50		0.24	0.30	0.98
40	0.0	0.05		0.28	1.08
	0.05	0.07		0.28	1.09
	0.10	0.09		0.29	0.92
	0.20	0.11	0.15	0.27	0.78
	0.30	0.13	0.17	0.32	0.78
	0.40	0.16	0.20	0.30	0.96
	0.50		0.23	0.32	0.98

Average values from at least five runs.

Sample-to-sample deviations: $r_\infty^i \pm 0.01$.

times as shown, for example, in Fig. 3 indicates that this is not completely correct, because at 40 mol% cholesterol short lifetime components can still be detected, even though the lipid system should be exclusively β-phase (Fig. 1). Nevertheless, the relative weight of the faster components is very small and, in addition, model calculations show that the main conclusions of this work would not be changed by using a much more complex associative model. In this way, the rotational correlation times (θ) and residual anisotropies (r_∞) of the probe in the α- and β-phases in Table 3 were obtained. The θ values are in the limit of the resolution of the experimental technique and, considering the approximations involved, will not be discussed further. The order parameters of the probe in the two phases, $\langle P_2 \rangle^{\alpha,\beta}$, computed from the r_∞ values, are shown in Fig. 7 for a constant temperature ($T = 30°C$) as a function of the cholesterol concentration. Considering the above noted limitations of the technique, there is a remarkable agreement between the values of these parameters and the expected equilibrium phase changes of the lipid mixture. Thus, the value of $\langle P_2 \rangle^\alpha$, which is virtually the same as that in the fluid phase of pure DMPC, remains almost unchanged (0.65 ± 0.05) up to 20 mol% cholesterol. Moreover, at 30% cholesterol only a single order parameter, $\langle P_2 \rangle^\beta$, is recovered, as would be expected from the single phase composition shown in Fig. 1. The $\langle P_2 \rangle^\beta$ value remains also relatively constant around 0.75 ± 0.05 within the equi-
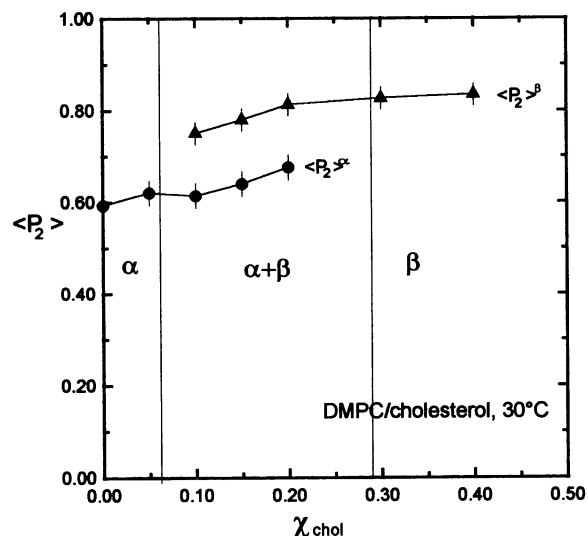

FIGURE 7 The order parameters of t-PnA in the α (●)- and β (▲)-phase of large unilamellar vesicles of DMPC at 30°C, as derived from the associative model.

librium range. This value is clearly higher than that of the α-phase (indicating important restrictions to the rotational mobility of the fluorescent probe) but lower than that recorded in a typical gel phase of a saturated lipid (0.95 for pure DMPC gel phase). When only the β-phase is present, $\langle P_2 \rangle^\beta$ shows a modest increase with cholesterol content.

It has been shown that the photophysical parameters of t-PnA are also sensitive to transient changes in the packing density of the bilayer lipids, with persistence times of tens of ns (Ruggiero and Hudson, 1989a). Fluctuations of this kind should also contribute to the experimental measurements presented above. Nevertheless, these data show quite convincingly that the fluorescence and anisotropy parameters of this probe can be of use in detecting and characterizing the α- and β-phases induced by cholesterol in the bilayer.

POPC/cholesterol

The maximum entropy analysis of the t-PnA fluorescence lifetime in pure POPC bilayers shows an apparent bimodal distribution, with a broad peak centered at ≈ 1 ns (Fig. 6). The lifetime analysis at $T < 30°C$ yields (Table 4) two fast components, with lifetimes of ≈ 1 and 2 ns, and a third medium one (6 ± 2 ns). This splitting of a single fast lifetime into two is also observed occasionally at higher temperatures and shows the physical limits of the numerical model used to analyze the decay curves. On the other hand, from the data in Table 4, it can be seen that the appearance of a long lifetime component ($\tau_4 = 10$–16 ns) is closely related to the cholesterol concentration of the bilayer. The amplitude of this component increases with the cholesterol molar fraction (Fig. 6) and is not correlated with the splitting of the short lifetime just discussed. Based on the experiments carried out in the mixed DMPC/cholesterol bilayer, this long lifetime can safely be assigned to the presence of a similar β-phase

above the transition temperature of POPC in the POPC/ cholesterol bilayer. The onset of formation of the β-phase at 30°C takes place at 5–10 mol% cholesterol, both in DMPC and in POPC (Fig. 6). As a first approximation here too, one may also assign the intermediate (6 ± 2 ns) and fast ($\approx$1 ns) lifetime components to the α-phase. As in the case of DMPC/ cholesterol mixtures, this is not a strictly correct procedure (see, e.g., Fig. 6), but other more accurate alternatives would increase the complexity of the model considerably without a corresponding gain in physical insight. Based on that simple assignment, we prepared bilayers that contained only α-phase or β-phase, by selecting the cholesterol concentration and temperature (α-phase: 5 mol% cholesterol, β-phase: 40 mol% cholesterol and 20°C) to determine the partition coefficient of t-PnA between the aqueous phase and each of the lipid phases, namely, K_p^α and K_p^β, following Sklar et al. (1979). The numerical values of these coefficients derived from fluorescence titration experiments (Sklar et al., 1980) are $K_p^\alpha = (3.5 \pm 1.0) \times 10^6$ and $K_p^\beta = (2.8 \pm 1.0) \times 10^6$. Thus, the partition coefficient of the fluorescent probe between the β- and α-phases of the POPC/cholesterol bilayer should be $K_p^{\beta/\alpha} = 0.8 \pm 0.5$, that is, there is little preferential solubility (if any) between the two phases.

In the previous discussion of DMPC/cholesterol bilayers, it was shown that, by combining the changes observed in the amplitude of the probe long lifetime component with the relative concentration of the α- and β-phases, as derived from the calorimetric phase diagram, it is possible to obtain an estimation of the probe partition coefficient between the two phases. In the case of POPC/cholesterol bilayers, one may use the same conceptual approach but in the reverse direction, to obtain the temperature/concentration relationship of the α- and β-phases from the changes in the amplitude of the probe long lifetime component, and the $K_p^{\beta/\alpha}$ value (0.8 ± 0.5) determined independently from fluorimetric titration. This is shown in Fig. 8 in the form of a thermal phase diagram, and it is interesting to note that its global features are similar to those of the DMPC/cholesterol phase diagram (Fig. 1). However, there is a very important difference in the location of $\alpha+\beta$ phase boundaries, because in the POPC/ cholesterol system at physiological temperatures both phases coexist well above 30% molar cholesterol. This finding may have biological relevance because, as indicated previously, unsaturated phospholipids form a major component of cell membranes. Moreover, it gives indirect support to the proposal that cholesterol may be an important, perhaps the major, factor responsible for the formation of heterogeneous lipid domains in some biological membranes (Gordon et al., 1984; Mateo et al., 1991).

Additional insight into the properties of the α- and β-phases in this bilayer can be obtained from the decay of the probe fluorescence anisotropy. In the case of POPC/ cholesterol bilayers, there is no rising anisotropy at long times as was observed in DMPC/cholesterol mixtures. However, because the fluorescence lifetime distribution profiles show the coexistence of different phases, we propose that the associative model described before provides a good physical
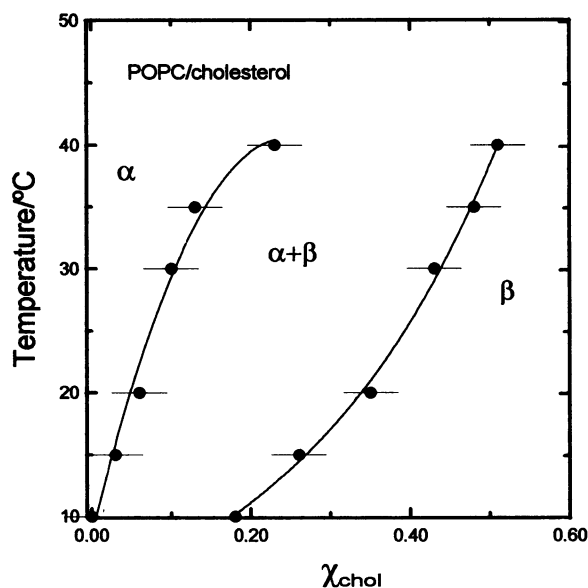
FIGURE 8   The distribution of the α- and β-phases in the POPC/ cholesterol system determined from the t-PnA lifetime analysis.

description of the mixed bilayers. According to that, the residual anisotropies and the corresponding order parameters for the probe in both phases, $\langle P_2 \rangle^{\alpha,\beta}$, were computed, as described above, as a function of cholesterol concentration at 30°C (Table 5 and Fig. 9). In the range of concentration where both phases coexist (10–40 mol% cholesterol), the two order parameters exhibit average values of $\langle P_2 \rangle^\alpha = 0.55 \pm 0.05$ and $\langle P_2 \rangle^\beta = 0.70 \pm 0.06$, but present (Fig. 9) a systematic upward drift, probably due to the limitations of the simple associative model used here. Nevertheless, it can be seen that $\langle P_2 \rangle^\beta$ is significantly lower than in the DMPC/
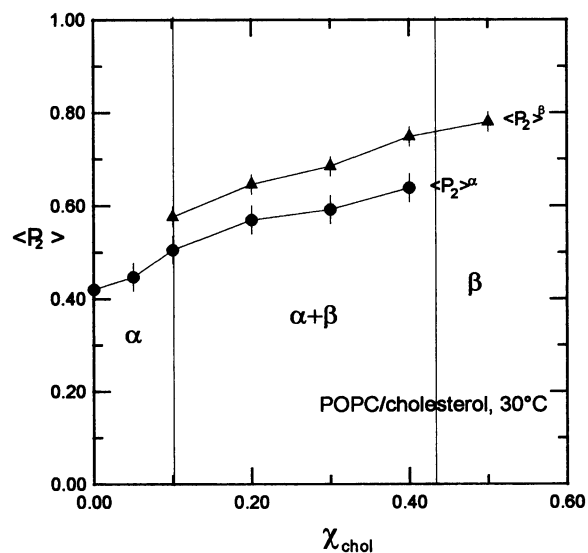
FIGURE 9   The order parameters of t-PnA in the α ($\bullet$)- and β ($\blacktriangle$)-phase of large unilamellar vesicles of POPC at 30°C, as derived from the associative model.

cholesterol system, indicating the importance of the structural distortion introduced in the lipid packing by the *cis* double bond of the unsaturated lipid.

CONCLUSIONS

The presence of liquid-disordered (α)- and a liquid-ordered (β)-phases characteristic of bilayers made up from DMPC/cholesterol can be detected from the changes induced in the fluorescence lifetimes of the lipophilic probe *t*-PnA. Specifically, it is shown that by associating the longest fluorescence lifetime with the probe population located in the β-phase it is possible to obtain a consistent picture of the changes in the relative concentration of the two phases as a function of cholesterol concentration and temperature. Based on this property of the fluorescent probe, it could be determined that bilayers made up from mixtures of POPC/cholesterol also show the presence of similar α- and β-phases for certain ranges of cholesterol concentration and temperatures above the POPC transition temperature. Furthermore, it could be determined that, in the POPC/cholesterol system, the two liquid-crystalline phases coexist up to 40 mol% cholesterol concentration in the physiological temperature range. Finally, from the residual anisotropy (or the order parameter) of the probe in each phase, the effects on long-range orientational order of cholesterol and lipid unsaturation in the lipid bilayer are demonstrated.

REFERENCES

Almeida, P. F. F., W. L. C. Vaz, and T. E. Thompson. 1992. Lateral diffusion in the liquid phases of dimyristoylphosphatidylcholine/cholesterol lipid bilayers: a free volume analysis. *Biochemistry.* 31:6739–6747.

Bloom, M., E. Evans, and O. G. Mouritsen. 1991. Physical properties of the fluid lipid-bilayer component of cell membranes: a perspective. *Q. Rev. Biophys.* 24:293–397.

Brochon, J. C. 1994. Maximum entropy method of data analysis in time-resolved spectroscopy. *Methods Enzymol.* 240:262–311.

Brochon, J. C., F. Merola, and A. K. Livesey. 1992. Time-resolved fluorescence study of dynamic parameters in biosystems. *In* Synchrotron Radiation and Dynamic Phenomena. American Institute of Physics, New York. 435–452.

Brochon, J. C., P. Tauc, F. Merola, and B. M. Schoot. 1993. Analysis of a recombinant protein preparation on physical homogeneity and state of aggregation. *Anal. Chem.* 65:1028–1034.

Cross, A. J., and G. R. Fleming. 1984. Analysis of time-resolved fluorescence anisotropy decays. *Biophys. J.* 46:45–56.

Gallay, J., and M. Vincent. 1986. Cardiolipin-cholesterol interactions in the liquid-crystalline phase: a steady-state and time-resolved fluorescence anisotropy study with cis and trans-parinaric acids as probes. *Biochemistry.* 25:2650–2656.

Gilbert, C. W. 1983. A vector method for the non-linear least squares reconvolution-and-fitting analysis of polarized fluorescence decay data. *In* Time-Resolved Fluorescence Spectroscopy in Biochemistry and Biology. R. B. Cundall and R. E. Dale, editors. NATO ASI series, Ser A: Life Sciences, Vol. 69. Plenum Press, New York. 605–606.

Gordon, L. H., P. W. Mobley, J. A. Esgate, G. Hoffman, A. D. Whetton, and M. D. Houslay. 1983. Thermotropic lipid phase separation in human platelet and rat liver plasma membrane. *J. Membr. Biol.* 76: 139–149.

Hudson, B. S., and S. A. Cavalier. 1988. Studies of membrane dynamics and lipid-protein interactions with parinaric acid. *In* Spectroscopic Membrane Probes, Vol. 1. L. M. Loew, editor. CRC Press, Boca Raton, FL. 43–62.

Hudson, B. S., D. L. Harris, R. D. Ludescher, A. Ruggiero, A. Cooney-Freed, and S. A. Cavalier. 1986. Fluorescence probe studies of protein and membranes. *In* Applications of Fluorescence in the Biomedical Sciences. D. L. Taylor, A. S. Waggoner, F. Lanni, R. F. Murphy, and R. Birge, editors. Alan R. Liss, Inc., New York. 159–202.

Hope, M. J., M. B. Bally, G. Webb, and P. R. Cullis. 1985. Production of large unilamellar vesicles by a rapid extrusion procedure. Characterisation of size distribution, trapped volume and ability to maintain a membrane potential. *Biochim. Biophys. Acta.* 812:55–65.

Ipsen, J. H., G. Karlström, O. G. Mouritsen, H. Wennerström, and M. J. Zuckermann. 1987. Phase equilibria in the phosphatidylcholine-cholesterol system. *Biochim. Biophys. Acta.* 905:162–172.

Ipsen, J. H., O. G. Mouritsen, and M. Bloom. 1990. Relationships between lipid membrane area, hydrophobic thickness, and acyl-chain orientational order. *Biophys. J.* 57:405–412.

Lentz, B. R., D. A. Barrow, and M. Hoechli. 1980. Cholesterol-phosphatidylcholine interactions in multilamellar vesicles. *Biochemistry.* 19:1943–1954.

Linseisen, F. M., J. L. Thewalt, M. Bloom, and T. M. Bayerl. 1993. ^{2}H-NMR and DSC study of SEPC-cholesterol mixtures. *Chem. Phys. Lipids.* 65: 141–149.

Livesey, A. K., and J. C. Brochon. 1987. Analyzing the distribution of decay constants in pulse-fluorimetry using the maximum entropy method. *Biophys. J.* 52:693–706.

Ludescher, R. D., L. Peting, S. Hudson, and B. Hudson. 1987. Time-resolved fluorescence anisotropy for systems with lifetime and dynamic heterogeneity. *Biophys. Chem.* 28:59–75.

Mabrey, S., P. L. Mateo, and J. M. Sturtevant. 1978. High-sensitivity scanning calorimetric study of mixtures of cholesterol with dimyristoyl- and dipalmitoylphosphatidylcholines. *Biochemistry.* 17:2464–2468.

Mabrey, S., and J. M. Sturtevant. 1976. Investigation of phase transitions of lipid mixtures by high sensitivity differential scanning calorimetry. *Proc. Natl. Acad. Sci. USA.* 73:3862–3866.

Mateo, C. R., J. C. Brochon, and A. U. Acuña. 1994. Effects of cholesterol on the packing density heterogeneity of phospholipid bilayers studied by *trans*-parinaric acid fluorescence decay. *Biophys. J.* 66: 286a. (Abstr.)

Mateo, C. R., J. C. Brochon, M. P. Lillo, and A. U. Acuña. 1993a. Lipid bilayer lateral clustering as detected by the fluorescence kinetics and anisotropy of *trans*-parinaric acid. *Biophys. J.* 65:2237–2247.

Mateo, C. R., M. P. Lillo, J. Gonzalez-Rodriguez, and A. U. Acuña. 1991. Lateral heterogeneity in human platelet plasma membrane and lipids from the time resolved fluorescence of trans-parinaric acid. *Eur. Biophys. J.* 20:53–59.

Mateo, C. R., P. Tauc, and J. C. Brochon. 1993b. Pressure effects on physical properties of lipid bilayers detected by *trans*-parinaric acid fluorescence decay. *Biophys. J.* 65:2248–2259.

Mortensen, K., W. Pfeiffer, E. Sackmann, and W. Knoll. 1988. Structural properties of a phosphatidylcholine-cholesterol system as studied by small angle neutron scattering: ripple structure and phase diagram. *Biochim. Biophys. Acta.* 945:221–245.

Naqvi, K. R. 1981. Photoselection in uniaxial liquid crystals: the advantages of using saturation light pulses for the determination of orientational order. *J. Chem. Phys.* 74:2658–2659.

Parasassi, T., M. DiStefano, M. Loiero, G. Ravagnan, and E. Gratton. 1994. Influence of cholesterol on phospholipid bilayers phase domains as detected by Laurdan fluorescence. *Biophys. J.* 66:120–132.

Pasenkiewicz-Gierula, M., W. K. Subczynski, and A. Kusumi. 1990. Rotational diffusion of steroid molecule in phosphatidylcholine-cholesterol membranes: fluid-phase microimmiscibility in unsaturated phosphatidylcholine-cholesterol membranes. *Biochemistry.* 29: 4059–4069.

Recktenwald, D. J., and H. M. McConnell. 1981. Phase equilibria in binary mixtures of phosphatidylcholine and cholesterol. *Biochemistry.* 20:4505–4510.

Reinl, H., T. Brumm, and T. M. Bayerl. 1992. Changes of the physical propeties of the liquid-ordered phase with temperature in binary mixtures of DPPC with cholesterol. *Biophys. J.* 1025–1035.

Ruggiero, A., and B. S. Hudson. 1989a. Critical density fluctuations in lipid bilayers detected by fluorescence lifetime heterogeneity. *Biophys. J.* 55: 1111–1124.

Ruggiero, A., and B. S. Hudson. 1989b. Analysis of the anisotropy decay of *trans*-parinaric acid in lipid bilayers. *Biophys. J.* 55: 1125–1135.

Sankaram, M. B., and T. E. Thompson. 1990. Interaction of cholesterol with various glycerophospholipids and sphingomyelin. *Biochemistry.* 29:10670–10675.

Sankaram, M. B., and T. E. Thompson. 1991. Cholesterol-induced fluid-phase immiscibility in membranes. *Proc. Natl. Acad. Sci. USA.* 88: 8686–8690.

Schroeder, F., J. R. Jefferson, A. B. Kier, J. Knittel, T. J. Scallen, W. Gibson, M. Wood, and I. Hapala. 1991. Membrane cholesterol dynamics: cholesterol domains and kinetics pools. *Proc. Soc. Exp. Biol. Med.* 196:235–252.

Scott, H. L. 1991. Lipid-cholesterol interactions. *Biophys. J.* 59:445–455.

Shang, Q.-Y., X. Dou, and B. S. Hudson. 1991. Off-axis orientation of the electronic transition moment for a linear conjugated polyene. *Nature.* 352:703–705.

Sklar, L. A. 1980. The partition of *cis*-parinaric acid and *trans*-parinaric acid among aqueous, fluid lipid and solid lipid phases. *Mol. Cell. Biochem.* 32:169–177.

Sklar, L. A., B. S. Hudson, R. D. Simoni. 1977. Conjugated polyene fatty acids as fluorescent probes: synthetic phospholipid membrane studies. *Biochemistry.* 16:819–828.

Sklar, L. A., G. P. Miljanich, and E. A. Dratz. 1979. Phospholipid lateral phase separation and the partition of *cis*-parinaric acid and *trans*-parinaric acid among aqueous, solid lipid, and fluid lipid phases. *Biochemistry.* 18:1707–1716.

Thewalt, J. L., and M. Bloom. 1992. Phosphatidylcholine: cholesterol phase diagrams. *Biophys. J.* 63:1176–1181.

Vist, M. R., and J. H. Davis. 1990. Phase equilibria of cholesterol/dipalmitoylphosphatidylcholine mixtures: ^{2}H nuclear magnetic resonance and differential scanning calorimetry. *Biochemistry.* 29:451–464.